

# Production of highly soluble foliar fertilizer in a spouted bed dryer

## Produção de fertilizante foliar de alta solubilidade em secador de leito de jorro

Ana Carolina Ribeiro Stoppe<sup>1</sup> , Mario Sérgio da Luz<sup>1</sup> , José Luiz Vieira Neto<sup>2</sup> , Kássia Graciele dos Santos<sup>1\*</sup> 

<sup>1</sup>Universidade Federal do Triângulo Mineiro/UFTM, Programa de Mestrado Profissional em Inovação Tecnológica/PMPIT, Uberaba, MG, Brasil

<sup>2</sup>Universidade Federal do Triângulo Mineiro/UFTM, Departamento de Engenharia Química/DEQ, Uberaba, MG, Brasil

\*Corresponding author: [kassia.santos@uftm.edu.br](mailto:kassia.santos@uftm.edu.br)

Received in January 11, 2023 and approved in April 5, 2023

### ABSTRACT

The drying process can be useful to change the particulate structure, improving the powder solubility. In this study, we investigated the drying of foliar fertilizer in a spouted bed using polyethylene pellets as inert particles to improve its solubility. A 2<sup>3</sup> factorial experimental design was used to evaluate how the powder yield and moisture were affected by the feeding time, intermittency time, and feed atomizer position. The spouting instability caused powder retention on the bed wall, which decreased the powder recovery efficiency by 2.3-26.6%. Although the powder recovery efficiency was low, the solubility time was reduced by 5.9 times, probably due to particle agglomeration, which increased the amorphous phase of the fertilizer. Design alterations, suggested by the CFD data, can increase spouted bed stability and facilitate centralized spouting. Based on this, the spouted bed drying technique was applied, and it effectively increased the solubility of commercial fertilizer, thus, incorporating more desirable characteristics for field applications.

**Index terms:** Drying pastes; inert particles; LDPE; solubility; CFD.

### RESUMO

O processo de secagem pode alterar a estrutura de sólidos, aumentando a solubilidade de pós. Este trabalho investigou a secagem de um fertilizante foliar em leito de jorro, empregando pellets de polietileno como sólido inerte, a fim de aumentar sua solubilidade. Utilizou-se um planejamento fatorial 2<sup>3</sup> para avaliar como a produtividade de pó e sua umidade foram influenciados pelo tempo de alimentação, tempo de intermitência a posição do bico atomizador dentro do leito. A instabilidade do jorro, causou a retenção de pó nas paredes do leito, o que conduziu a baixas eficiências de recuperação de pó (2,3 a 26,6%). Foram propostas alterações na geometria do leito, baseadas nas simulações CFD, a fim de aumentar a estabilidade do leito e centralização da fonte. Apesar da baixa produção de pó, a solubilidade foi reduzida em 5,9 vezes, provavelmente devido à aglomeração e aumento da fase amorfa na estrutura do pó. Assim, a secagem em leito de jorro foi efetiva em aumentar a solubilidade do fertilizante, incorporando uma característica atrativa à sua aplicação nas lavouras.

**Termos para indexação:** Secagem de pastas; partículas inertes; polietileno; solubilidade; CFD.

## INTRODUCTION

To meet the demands of an ever-growing population, farmers must increase their food production by adopting different strategies, including new technologies and techniques, such as the use of efficient fertilizers. Foliar fertilization is an efficient method of supplementing soil nutrients and can be especially useful when soil fertility is low or under harsh environmental conditions (Aghaye Noroozlo et al., 2019).

Foliar fertilizers are usually sprayed on the leaves of plants and are quickly absorbed. These fertilizers are usually marketed as powders, which reduces the cost of transportation. They need to be dissolved in water by the farmer before being applied to the crops (Ferraz et al., 2021). Fertilizers and insecticides are frequently mixed for

field application which can reduce solubility and clog spray nozzles (Alberto et al., 2022). Thus, making foliar fertilizers more soluble might add value to the product and decrease operational costs. Foliar feeding has specific rules that should be followed by farmers to prevent any problems from arising (Dehnavard; Souri; Mardanlu, 2017; Souri; Hatamian, 2019).

Some techniques are commonly used to dry pastes and solutions, such as spray dryers, lyophilizers, fluidized bed dryers, and spouted bed dryers (Mujumdar, 2014). Although the industrial application of these techniques for drying pastes and solutions is widespread, studies involving fertilizers are limited. Alberto et al. (2022) investigated the drying of an aqueous fertilizer solution using the spray drying technique. The product showed a reduction of 90.2% on the initial solubility time because of the capillary effects caused by the high porosity, roughness, and agglomeration of the particles.

Spouted beds produce a product whose quality is similar to those obtained by spray dryers and fluidized techniques but at a lower cost and higher water evaporation rate (Barros; Freire, 2019). In the process, solutions and pastes are atomized or drizzled onto the inert particle bed, and they act as suspension support. Then, a thin layer of paste wets the particle surfaces, causing rapid drying. The intense particle collisions in the spouted bed promote the removal of dry matter in powder form, which is elutriated by the air and collected in a cyclone (Dantas et al., 2018).

Selecting the appropriate conditions for the process is crucial for satisfactory drying efficiency. Many factors can influence the heat and mass transfer during the drying process, including airflow, the paste flow rate, temperature, feeding intermittency, properties of inert particles, and spouted bed fluid dynamics. According to Dantas et al. (2018), the feed should be intermittent to prevent the bed from collapsing, especially with a high flow of the paste. Thus, the time intervals with or without feeding can reduce the moisture, which prevents particle agglomeration, promotes bed stability, and enhances powder production efficiency.

To evaluate whether a solution or paste can efficiently wet the surface of a particle, the contact angle between them needs to be considered. Rocha, Donida and Marques (2009) found that contact angles greater than  $70^\circ$  do not contribute to the coating of the particle. This happens because the adhesion forces of the polymeric film on the surface of the inert solid are weak, the paste dries and forms granules, and the fine powder gets eluted by the process.

Although spouted beds have many advantages for the drying of pastes, the powder production rate using spouted beds is lower than that recorded by using other industrial equipment. The spouted bed might be unstable due to particle agglomeration and powder accumulation within the bed. Therefore, further studies are needed to overcome the operational limitations of spouted bed dryers (Passos; Mujumdar, 2000).

Regarding the stability of spouted beds, San José et al. (1998) measured the solid flow rate using an optical fiber at different longitudinal points along the spout to quantify the solid crossflow in conical spouted beds. According to them, a ratio of the gas inlet diameter ( $D_o$ ) to the contactor base diameter ( $D_i$ ) of 1:2 shows the maximum solid circulation rate while maintaining bed stability and a low pressure drop. Thus, the drying application requires a vigorous regime and a longer trajectory of the solid in the contactor. An contactor angle of  $45^\circ$  produces the highest solid circulation rate, with solids defining a broader trajectory.

Some researchers have investigated the effect of operating conditions on powder retention in spouted bed dryers with inert particles. Vieira et al. (2019) investigated the effects of air inlet temperature and the paste inlet flow rate disturbances on milk paste drying in a spouted bed. The moisture in milk powder was measured using a soft sensor. Powder retention in the spouted bed was greater at longer drying periods, which reduced the accuracy of the moisture soft sensor. These findings highlighted the importance of developing a novel approach for modeling paste drying to better describe paste accumulation within the bed.

A novel fountain confiner device was recently developed to reduce fine particle entrainment and maximize solid-gas contact, which is a critical parameter for drying. Altzibar et al. (2017) found a 60-70% reduction in fine particle entrainment and a decrease in the operating bed pressure drop and particle maximum cycle duration. The stability of the fountain increased considerably, which homogenized the solid circulation in the bed.

Estiati et al. (2019) dried small sand particles in a conical spouted bed with a draft tube and a fountain confiner. The findings showed a significant reduction in the drying time, pressure drop, and airflow rate. The open-sided draft tube outperformed all other configurations concerning the drying performance and required the minimum drying time. Because of their weak gas-solid interactions, nonporous draft tubes were the poorest option. An intermediate level of performance was achieved with porous draft tubes.

Brito et al. (2021) investigated the drying of alumina, barley, and soybean particles in a conical spouted draft tube bed. They found that the efficiency of energy consumption and drying depends on the dryer design, the operating parameters, and the properties of solids. Internal draft tubes can limit air percolation and result in inferior gas-solid interactions. Consequently, the energy consumption was lower when a diffusive material was used, which exhibited a significant loss of moisture compared to other materials.

Sukunza et al. (2022) presented a model for estimating heat and mass transfer coefficients in a spouted bed with a confiner device. The findings showed that raising the inlet air temperature decreased airflow turbulence around the particle, thus, lowering the mass transfer coefficient. Also, because of inadequate air and particle circulation, a drop in air velocity lowered the mass transfer coefficient.

The main issue with foliar fertilization is the low solubility of the fertilizer or its incompatibility with pesticides, which causes precipitation and clogging of spray nozzles. Drying procedures can modify the structure of the fertilizer, increasing its solubility and reducing issues with field application.

In this study, we described the drying of commercial fertilizer in a spouted bed dryer operating with inert particles. A factorial design was used to evaluate the effect of the solution feeding time, intermittence time, and the feed atomizer position on drying efficiency. Qualitative Computational Fluid Dynamics - CFD simulations were performed to elucidate the changes in bed geometry for improving the spouting stability. We also evaluated the dryer capacity regarding powder yield, moisture, and solubility.

## MATERIAL AND METHODS

### Characterization of the foliar fertilizer

The commercial powder foliar fertilizer (PFF) used in this study was a source of micronutrients consisting of 16.5% S, 0.50% B, 1.00% Cu, 25.0% Mn, and 4.00% Zn, with acidity between 2.80 and 3.80. The same fertilizer was dried by Alberto et al. (2022).

Granulometric analyses of PFF and dried powder foliar fertilizer (D-PFF) were performed by sieving using standard Tyler series sieves with 40, 45, 50, 100, and 270 mesh and estimating the average diameter of Sauter from both samples in triplicate.

The moisture tests of the PFF and D-PFF samples were performed in an oven at 105 °C for 24 h to evaluate the drying efficiency.

To assess the fertilizer quality, we performed the solubility test for PFF and D-PFF samples. Initially, 0.5 g of fertilizer was weighed on the analytical balance and mixed with 25 mL of distilled water under agitation at 720 rpm (Brasil, 2016). The time needed to obtain a translucent/translucent solution was recorded, which allowed us to visualize an internal vortex (Alberto et al., 2022).

The identification of the structures in the samples before and after drying was performed using X-ray powder diffraction (XRD) (PANalytical model Empyren) using Cu K $\alpha$  radiation.

Morphological characterization of PFF and D-PFF samples was performed using an optical microscope with a magnification of 1,600x.

### Characterization of the inert solid

We used low-density polyethylene pellets (LDPE) as inert particles. The LDPE particles had a mean diameter of 4 mm and an apparent density of 878 kg/m<sup>3</sup>. Thus, it was in the D group as per the Geldart classification and was suitable for spouting.

To ensure that the LDPE particles were suitable, we measured the contact angle between a drop of foliar fertilizer

solution and the surface of LDPE. We analyzed about 40 photos of drops on a flat LDPE surface using a solution of fertilizer with 0.5 kg/L. Then, the photos were analyzed on the Online Transfer website (Ginifab, 2021), as shown in Figure 1.

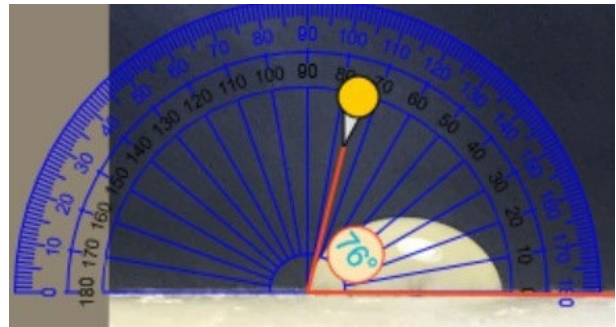


**Figure 1:** The contact angle between a drop and the LDPE flat surface was measured on the Online Transfer website.

The measured contact angle was 76.22°, indicating that the liquid solution could wet the LDPE surface, as the contact angle was less than 90°. Additionally, as the contact angle was greater than 70°, it was suitable for bed drying granulation, based on the findings of Rocha, Donida, and Marques (2009).

### Experimental unit

The drying experiments were conducted in a stainless-steel cone-cylindrical spouted bed with an internal angle of 40°. The diameter of the cylindrical section ( $D_c$ ) and the gas inlet diameter ( $D_o$ ) were 0.12 m and 0.02 m, respectively. The spouted bed geometry (a) and a schematic representation of the experimental apparatus (b) are shown in Figure 2.

An air blower provided the air (4 hp). The air was heated using a 4,000 W resistance controlled by a PID controller. An orifice flow meter was used to measure the airflow rate, and differential pressure transducers were used to monitor the pressure drop across the orifice. The pressure drop through the particle bed was monitored using a pressure transducer (Series MS Magnesense® from Dwyer Instruments), and the signal was sent to a microcomputer through an A/D data acquisition card (National Instruments DAQ - USB 6001) and processed using the LabVIEW software.

The temperature was monitored by thermocouples along the bed at three different positions (heights) on the cylinder bed. The fertilizer solution was sprayed using a dual-fluid atomizing nozzle; one was connected to the peristaltic pump, and the other was connected to the air compressor hose that worked at 1 bar.

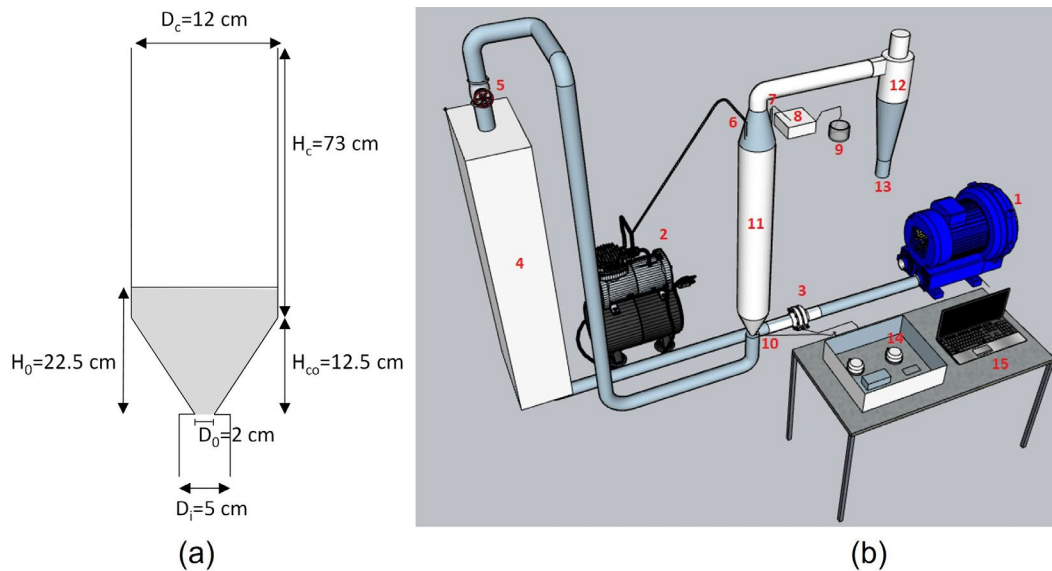


**Figure 2:** Spouted bed geometry (a) and experimental unit scheme (b): (1) Drying air blower; (2) Atomizing air compressor; (3) Orifice plate and flow meter; (4) Heating system; (5) Gate valve to control the drying air flow; (6) Atomizing air inlet; (7) Solution power inlet; (8) Peristaltic Pump; (9) Beaker with the fertilizer solution; (10) Bed pressure drop gauge; (11) Spouted bed; (12) Cyclone; (13) Product collection point (cyclone underflow); (14) Data acquisition system; (15) Computer.

The dried fertilizer was elutriated and collected in a Lapple cyclone with a cylindrical diameter of 0.105 m. A bag filter (200 mesh) was added at the cyclone overflow to collect the fine particulate matter.

### Spouted bed fluid dynamics

The operational airflow rate for the drying experiments was fixed based on the experimental characteristic curve of the spouted bed loaded with 1 kg of LDPE particles. The minimum spouting condition was obtained by plotting the pressure drop as a function of decreasing inlet air velocity and by the visual monitoring of the movement of the particles on the bed surface (Santos et al., 2019). The point at which the spout collapsed was defined as the minimum spouting airflow rate ( $Q_{ms}$ ) and pressure drop ( $\Delta P_{ms}$ ). Thus, the operational airflow rate ( $Q$ ) was 1.5 times greater than  $Q_{ms}$  (Pereira; Godoi; Rocha, 2010).

The spouted bed fluid dynamics were simulated using the CFD technique to verify the spouting stability at the operational airflow rate.

We simulated the original configuration (OC) of the spouted bed to study the sources of instabilities after early experimental testing revealed unstable spouting. Then, we simulated an alternative configuration (AC) with a conical contactor under the bottom, as proposed

by Olazar et al. (1992). The initial height of the static bed was 0.225 m, with a voidage of 0.39.

The simulations were performed using the Fluent® program. We adopted the Eulerian multiphase model TFM (Two-Fluid Model) to simulate the fluid dynamic behavior of a spouted bed containing LDPE particles. The simulation strategy and the mathematical model used in this study were validated by Duarte et al. (2005), and many studies have used it to represent spouted bed fluid dynamics (Santos; Murata; Barrozo, 2009; Santos et al., 2012; Santos et al., 2017). A 2D computational mesh of both geometries was created using the Gambit® software. The mesh of the OC configuration with 7,400 quadrilateral elements is shown in Figure 3a, and the spouted bed with a conical contactor under the bottom, composed of about 10,851 quadrilateral elements, is shown in Figure 3b.

The system that included the continuity and momentum transfer equations for the fluid and granular phases was solved using the Finite Volume Method. The SIMPLE Algorithm was used to establish the velocity-pressure coupling. We simulated about 5 s of real-time and found a convergence tolerance of  $1 \times 10^{-3}$  (Santos et al., 2012; Araújo; Santos, 2017).

The bed geometry values and the experimental and simulated conditions used for the spouted bed computational fluid dynamics are presented in Table 1.

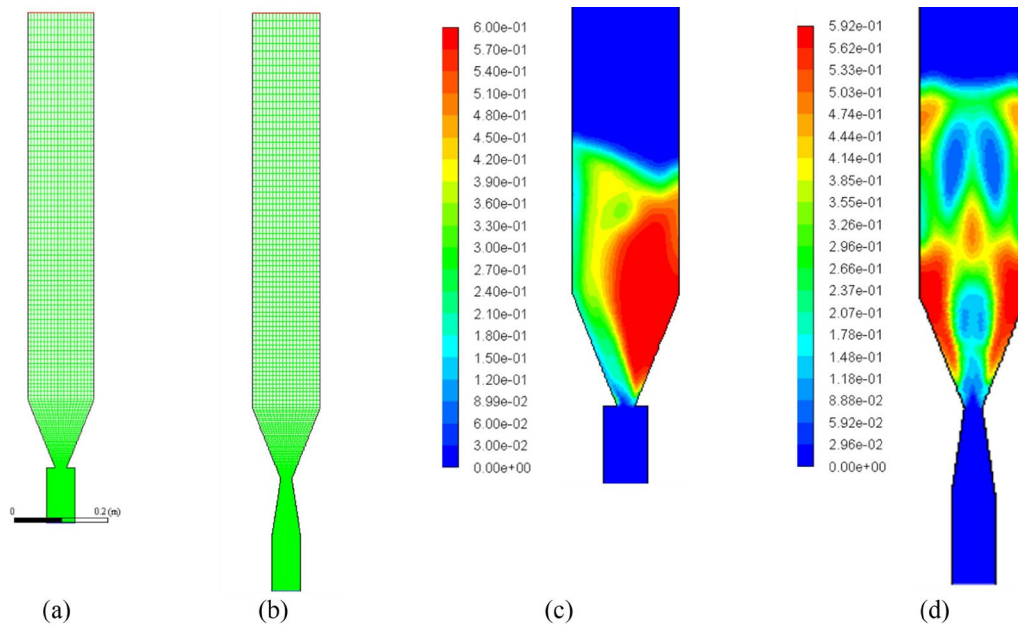


**Figure 3:** Mesh designed for CFD simulation of OC configuration (a) and AC configuration (b); contours of solid volume fraction for OC configuration (c) and AC configuration with a conical contactor (d).

**Table 1:** Spouted bed geometry and operational conditions used in CFD simulations.

Spouted bed geometry	Experimental conditions used in CFD simulations
$D_0 = 0.05$ m	Particle density 878 kg/m <sup>3</sup>
$D_i = 0.02$ m	Particle diameter 0.004 m
$H_{co} = 0.125$ m	Particle loading 1 kg
$H_{co} = 0.73$ m	Voidage 0.39
$D_c = 0.12$ m	Air low rate ( $Q_{1.5ms}$ ) 120 m <sup>3</sup> /h
$H_0 = 0.225$ m	Time step $1 \times 10^{-3}$ s

### Drying experiments

To define the operating ranges of the experimental unit, we conducted preliminary tests, such as the evaluation of the pump flow and the pressure of the atomizer nozzle. The results of the preliminary tests showed that the bed had high relative humidity inside when it was operated in continuous solution feed. Dantas et al. (2018) showed that the intermittent feeding of the solution is an alternative, as it provides better fluid dynamics in the system, reducing moisture and particle agglomeration, thus improving drying.

All experiments were performed using about 1 kg of LDPE particles, an air supply flow rate of 120 m<sup>3</sup>/h (about 1.5x Qms), a feeding flow rate of 19 mL/min, an atomizer nozzle pressure of 1 bar, and a drying air temperature of 100 °C.

The tests were designed according to a 2<sup>3</sup> factorial design to evaluate the effect of three factors on several responses, including feeding time ( $t_f$ ), intermittent suspension feeding time ( $t_i$ ), and feed atomizer position ( $H_a$ ), using Equation 1, 2 and 3, respectively.

$$x_1 = \frac{t_f - 20s}{10s} \quad (1)$$

$$x_2 = \frac{t_i - 180s}{120s} \quad (2)$$

$$x_3 = \frac{H_a - 0.54m}{0.14m} \quad (3)$$

Multiple regression was performed to evaluate the whole set of experimental data and assess the impact of each independent variable on the responses, i.e., powder yield ( $h$  [%]) and moisture ( $M$  [%]). The Student's  $t$ -test was performed to determine the significance of the regression parameters ( $p < 0.1$ ).

For drying, the air was heated up to the specified temperature, and then the paste was injected. About 100 mL of the PFF aqueous solution (0.5 kg/L) was fed based on the feeding time and intermittent suspension feeding time, which were defined by the experimental design. The fluid was then evaporated to produce the dried powder foliar fertilizer (D-PFF).

The powder yield was calculated using Equation 4, as the ratio of the mass of dry powder collected in the underflow of the cyclone ( $m$ ) to the initial mass of the fertilizer in the feed solution ( $m_0$ ).

$$\eta = \frac{m}{m_0} \cdot 100 \quad (4)$$

## RESULTS AND DISCUSSION

### Fluid dynamics of the spouted bed

The experimental characteristic curve of pressure drops as a function of airflow for a bed loaded with 1 kg of LDPE particles is shown in Figure 4. The minimum

spouting was observed at  $Q_{ms} = 80 \text{ m}^3/\text{h}$ , which led to a pressure drop ( $-\Delta P_{ms} = 817 \text{ Pa}$ ). Thus, the operational airflow rate for the drying tests was set at  $120 \text{ m}^3/\text{h}$ .

Although the characteristic curve had a conventional shape, the bed exhibited unstable spouting, which was directed toward the wall of the equipment and was not centralized. This affected the powder yield during drying since the wet particles were thrown on the wall before the drying was completed, which caused powder adhesion to the bed wall.

The results of the simulation confirmed the experimental observations for the OC configuration, as shown by the volumetric fraction contour of the solids in Figure 3c, in which the unstable spouting was visible. The fountain was displaced to the bed wall rather than being firmly attached to the center of the bed.

Olazar et al. (1992) described a similar behavior for the spouting of glass sphere particles less than 6 mm in diameter, where the jet projected the particles vertically. They also found that the ratio of the gas inlet diameter ( $D_0$ ) to the contactor base diameter ( $D_i$ ) should be  $\frac{1}{2} < D_0/D_i < 5/6$ . The upper limit relates to the undefinition of the fountain, which occurs when this ratio is very high and increases the instability owing to rotational motions. These findings explain the spout instability observed in the experiment for the conventional spouted bed since the value of  $D_0/D_i$  was 2.5, which was considerably higher than the indicated upper limit.

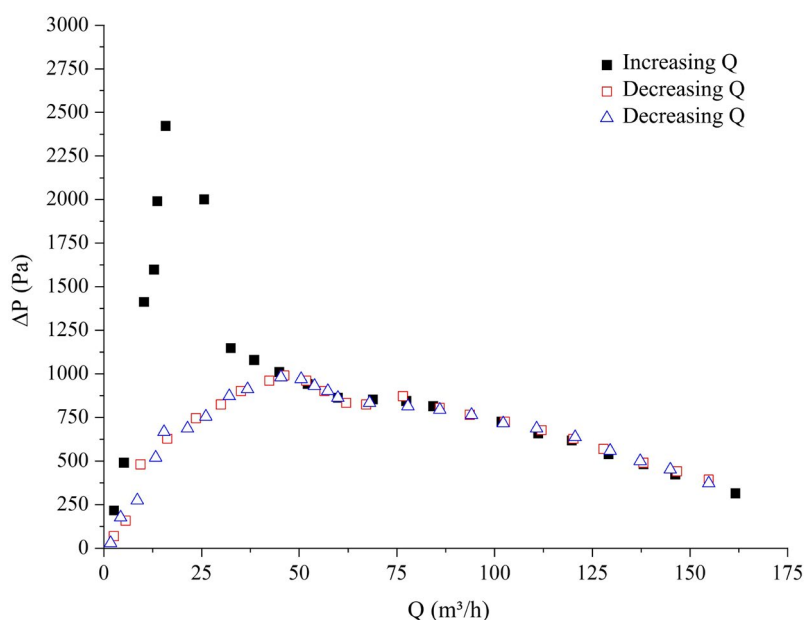


**Figure 4:** The characteristic curve of the spouted bed operating with 1 kg of inert LDPE particles.

The bed instability can be easily solved by inserting a new device to change the  $D_o/D_i$  ratio. The AC configuration had a  $D_o/D_i$  value of 1, which was close to the upper limit and could be a low-cost solution to improve the spouting stability. The simulated result for the AC configuration (Figure 3d) showed the centralized and stable spout, indicating that this new configuration could prevent the loss of powder that decreased the yield due to the retention of the solid at the bed wall.

### Drying experiments

The  $2^3$  factorial design in both original and coded variables, as well as, the primary responses studied, i.e., yield (h) and moisture (M), are shown in Table 2. All responses were evaluated individually by performing an ANOVA with a significance level of less than 10%. The significant effects on the main responses are presented in Table 3.

### Powder yield

The powder production efficiency of D-PFF in spouted bed dryers was between 2.3% and 26.6% (Table 2). These findings were different from those obtained in the spray dryer (67–82%), as reported by Alberto et al. (2022); thus, we recorded a lower powder yield of foliar fertilizer. At the end of the experiment, we observed high solid retention at the spouted bed wall and the cyclone wall, as well as on the surface of the particles. The instability of the spouting regime observed previously in the simulations compromised powder recovery. Thus, we speculated that changing the geometry of the spouted bed bottom might

increase the bed's fluid dynamic stability, which might directly affect the powder yield by decreasing its adhesion to the bed walls.

The drying process in the spouted bed with inert particles presented a moderate solid recovery, with dust recovery above 40% (Barros; Freire, 2019). A wide range of powder efficiency production was reported in different studies, including 0–50% for fruit paste (Medeiros et al., 2002; Rocha et al., 2011), 9–34% for milk-blackberry pulp (Braga; Rocha, 2013), 28–54% for pulp fruit mixture (Dantas et al., 2018), 11–53% for calcium carbonate paste with 5.0% m/m (Barros; Ferreira; Freire, 2019).

The results of the ANOVA (Table 3) revealed that the powder yield was affected by the intermittent suspension feeding time ( $x_2$ ) followed by atomizer height ( $x_3$ ) and also the interaction between the factors ( $x_2 \times x_3$ ), as shown in Figure 5a.

The highest yield was obtained when the feeding period was 30 s ( $x_1 = +1$ ), with a feeding pause of 60 s ( $x_2 = -1$ ) and a height of 0.68 m between the atomizer and the bottom ( $x_3 = +1$ ). The effect of  $x_3$  on powder efficiency production was positive, which implied that a higher feed atomizer position produced a larger amount of D-PFF.

Under these conditions, we also observed low retention of the powder on the inert surface, which contributed to the increase in yield. The adhesion of the solid on the bed wall was lower at  $Ha = 0.40$  m since the spray reached the inert particles directly. This indicated that at  $Ha = 0.68$  m, several droplets were elutriated to the cyclone before reaching the particle surface.

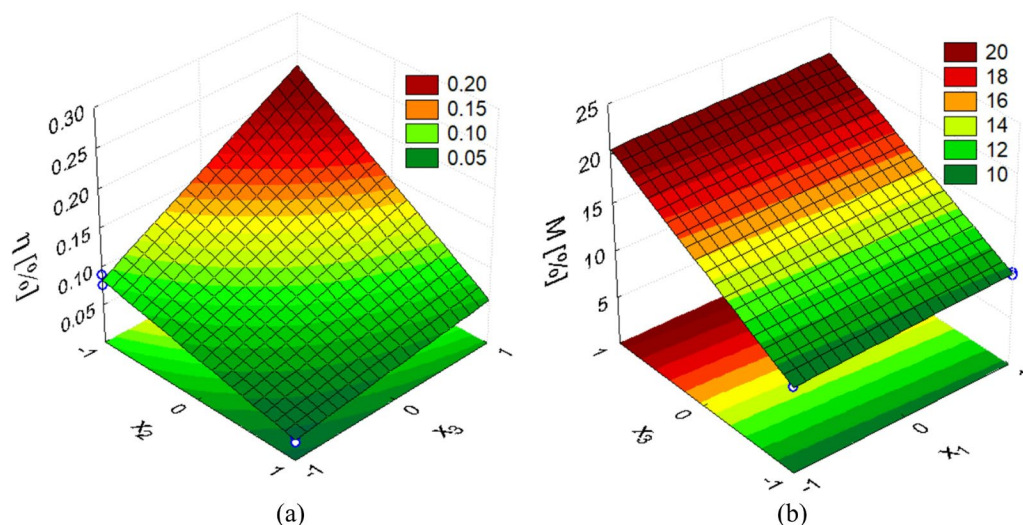
**Table 2:** Factorial design  $2^3$ : factors  $x_1$  (feeding time  $-t_f$ ),  $x_2$  (intermittent suspension feeding time  $-t_i$ ),  $x_3$  (the feed atomizer position  $-H_o$ ), and the results of yield ( $\eta$ ), productivity (P), and moisture (M) of the D-PFF.

Experiment	Factors			Responses	
	$t_f$ [s] ( $x_1$ )	$t_i$ [s] ( $x_2$ )	$H_o$ [m] ( $x_3$ )	h [g/g]	M [%]
1	10 (-1)	60 (-1)	0.40 (-1)	0.089	9.06
2	30 (+1)	60 (-1)	0.40 (-1)	0.076	9.77
3	10 (-1)	300 (+1)	0.40 (-1)	0.029	8.93
4	30 (+1)	300 (+1)	0.40 (-1)	0.023	9.48
5	10 (-1)	60 (-1)	0.68 (+1)	0.182	20.56
6	30 (+1)	60 (-1)	0.68 (+1)	0.252	21.78
7	10 (-1)	300 (+1)	0.68 (+1)	0.066	20.25
8	30 (+1)	300 (+1)	0.68 (+1)	0.049	21.44
9*	30 (+1)	60 (-1)	0.68 (+1)	0.266	20.53

\*Experiment 9 is a replicate of Experiment 6.

**Table 3:** The estimated effects were determined by ANOVA for the responses, including yield ( $\eta$ ) and moisture (M).

Responses	Factor	Effect	Deviation	p-level
h [g/g] ( $R^2= 0.939$ )	mean	0.100	0.010	0.000
	$x_2$	-0.116	0.020	0.002
	$x_3$	0.091	0.020	0.006
	$x_2 \times x_3$	-0.060	0.020	0.030
M [%] ( $R^2= 0.999$ )	mean	15.074	0.135	0.000
	$x_1$	0.747	0.270	0.032
	$x_3$	11.527	0.270	0.000

**Figure 5:** Response surface showing the influence of feeding time ( $x_1$ ), intermittent suspension feeding time ( $x_2$ ), and the feed atomizer position ( $x_3$ ) on the powder yield ( $\eta$ ) and moisture (M) of the D-PFF.

The intermittence time factor ( $x_2$ ) negatively affected the yield, showing that tests with long pause intervals between feedings did not increase the drying rate. Dantas et al. (2018) reported similar findings attributed to the longer processing time necessary to produce a specific volume of powder.

The feeding time range used in this study (10 s to 30 s) did not influence powder production. Hence, we speculated that the amount of paste within the bed was low, which might have contributed to an increase in the adhesion on the particle surface and the spouted bed wall. The extended periods without feeding resulted in a decrease in powder production because the particles were dried mainly by atomization, without interaction with the inert particle.

Therefore, we speculated that the design alterations suggested by the CFD data could increase the stability

of the spouted bed and provide centralized spouting. It might help to decrease the loss of powder on the bed wall. Higher values of feeding time can minimize the fraction of powder retained on inert surfaces and hence, boost powder production.

### Moisture content

According to Brazilian legislation, the maximum moisture of organomineral fertilizers has been standardized for soil application only, with the moisture up to 30% (Brasil, 2009).

The final moisture of D-PFF was between 8.9% and 21.8% (w.b.) (Table 2). The results of the statistical analysis (details in Table 3) showed that factors  $x_1$  and  $x_3$  affected the powder moisture. The drying was more effective when the feeding time and the atomizer height were low.

As the solution mostly consisted of water (~98%), an increase in the solution feeding time ( $x_1$ ) affected the powder moisture directly, resulting in higher humidity within the bed and the final product. According to Dantas et al. (2018), a smaller dryer capacity is used at low solution feed rates, which results in a better drying rate and minor alterations in the bed temperature. Thus, at a constant temperature, the greater the quantity of solution inside the bed, the greater the humidity of the final product. Barros and Freire (2019) also found that a lower feed flow resulted in lower humidity in the equipment, indicating that the maximum capacity of drying was not reached.

The height or position of the atomizer ( $x_3$ ) was the main factor influencing the powder moisture. The effect was positive, producing wet powder at  $H_a = 0.68$  m. This finding indicated that the spray was far from the inert particles and decreased its interaction between the solution. Thus, the powder did not adhere to the surface of the particles long enough to dry, being elutriated into the cyclone at higher humidity.

### Characterization of foliar fertilizer

The size distribution of PFF and D-PFF was obtained by sieving, and it was well-adjusted by the RRB model according to Equations 5 and 6, with  $R^2 = 0.999$  and  $0.978$ , respectively. The parameter  $D_{63}$  increased from 180  $\mu\text{m}$  to 240  $\mu\text{m}$  after the drying process.

$$X_{PFF} = 1 - \exp \left[ - \left( \frac{D}{180.3 \mu\text{m}} \right)^{4.286} \right] \quad (5)$$

$$X_{D-PFF} = 1 - \exp \left[ - \left( \frac{D}{240 \mu\text{m}} \right)^{1.740} \right] \quad (6)$$

The images of the two fertilizer powders (PFF and D-PFF) at a magnification of 1,600x are shown in Figure 6. We found that the particle size increased after drying, with particle sizes ranging from 27  $\mu\text{m}$  to 500  $\mu\text{m}$ .

The D-PFF was a polydisperse agglomerated particle with an irregular flake shape (Braga; Rocha, 2013). This agglomeration occurred probably because of random particle collisions in the atomizer cloud or due to the adhesion between the particles (Westergaard, 2004). During drying, a thin layer of paste was formed and continuously dried on the inert surface until the coating layer broke off as flakes or lumps because of interparticle friction and particle-wall collisions (Barros; Ferreira; Freire, 2019).

The solubility test was performed before and after the fertilizer underwent drying. The PFF dissolved in 112 s, while the D-PFF dissolved completely in 19 s. Thus, the D-PFF solubilized 5.9 times faster than the PFF.

This increase in solubility might be due to the new shape and particle structure. By enabling water penetration between the agglomerates and improving capillary-driven water flow into the agglomerate pores, agglomeration significantly improved the powder reconstitution properties and decreased the wetting time, thus, increasing solubility (Gong et al., 2008).

Alberto et al. (2022) found similar results for drying the same PFF in a spray dryer. The powder they obtained had a solubilization time between 11 s and 31 s.

The high powder solubility after drying might be due to structural alterations. The results of the XRD analysis are shown in Figure 7, where the fertilizer structure is compared before and after drying in SB. The results indicated that the level of crystallinity of D-PFF was lower.

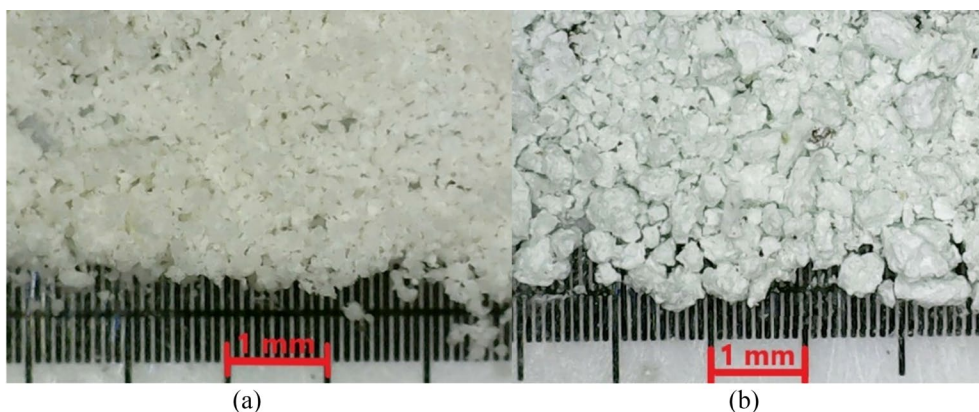


**Figure 6:** Images of fertilizers: (a) PFF and (b) D-PFF; magnification: 1,600x.

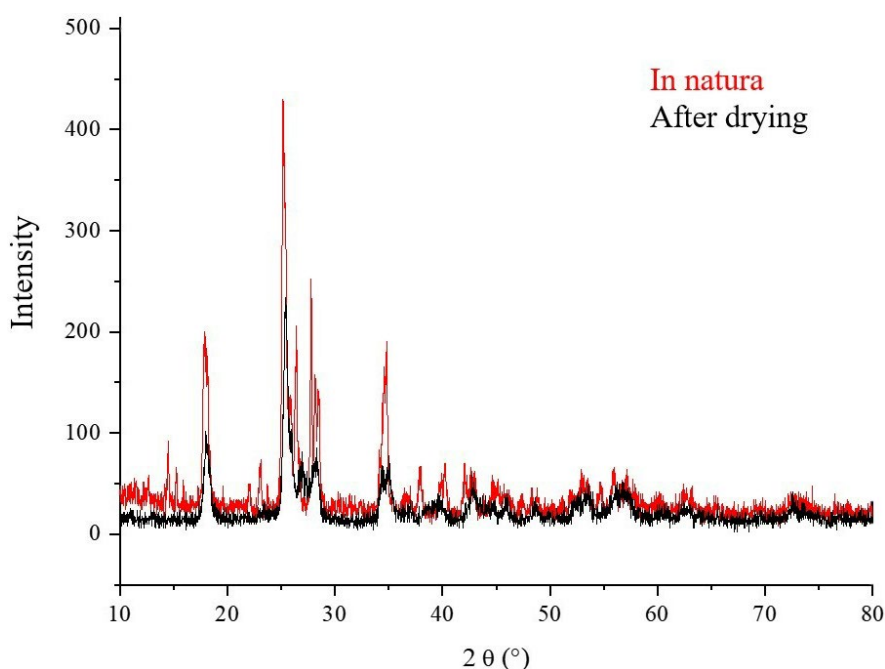


**Figure 7:** Overlap of the XRD curves of PFF and D-PFF.

The amorphous structures increased throughout the drying process, as shown in Figure 7. Because amorphous materials have stronger solvation qualities than crystalline materials, this alteration might have increased solubility. Souza et al. (2016) dried a cashew solution in a spouted bed, and the results of the XRD analysis of the final product showed that the powder had a more amorphous appearance.

Our findings showed that the spouted bed dryer enhanced the solubility of the commercial foliar fertilizer. However, the operational conditions of the drying process that can help maintain the fluid dynamic stability need to be investigated to reduce the loss of powder and maximize its productivity.

## CONCLUSIONS

The spouted bed dryer effectively decreased the solubilization time by 5.9 times. Powder recovery was low (<22.6%) due to the instability of the fountain and powder retention on the bed walls. The qualitative CFD results showed that the bed geometry alterations decreased the instability. Hence, we recommend that future studies should use the alternative configuration proposed in this study. We also suggest a shorter distance between the spray nozzle and the bottom to avoid dragging wet particles into the cyclone.

## AUTHOR CONTRIBUTION

Conceptual Idea: Santos, K.G.; Methodology design: Stoppe, A.C.R.; Vieira Neto, J.L.; Santos, K.G.; Data collection: Stoppe, A.C.R.; Data analysis and interpretation: Stoppe, A.C.R.; Da Luz, M.S.; Vieira Neto, J.L.; Santos, K.G.; and Writing and editing: Stoppe, A.C.R.; Da Luz, M.S.; Santos, K.G..

## ACKNOWLEDGEMENTS

The authors wish to thank the Professional Master's Programme in Technological Innovation of UFTM, Capes and the financial support by CNPq (Universal 433958/2018-9).

## REFERENCES

- AGHAYE NOROOZLO, Y.; SOURI, M. K.; DELSHAD, M. Effects of foliar application of glycine and glutamine amino acids on growth and quality of sweet basil. *Advances in Horticultural Science*, 33(4):495-501, 2019.
- ALBERTO, A. et al. Enhanced solubility of foliar fertilizer via spray dryer: Process analysis and productivity optimization by response surface methodology. *Ciência e Agrotecnologia*, 46:e002422, 2022.

- ALTZIBAR, H. et al. Fountain confined conical spouted beds. *Powder Technology*, 312:334-46, 2017.
- ARAÚJO, B. S. A.; SANTOS, K. G. CFD simulation of different flow regimes of the spout fluidized bed with draft plates. *Material Science Forum*, 899:89-94, 2017.
- BARROS, J. P. A. A.; FERREIRA, M. C.; FREIRE, J. T. Spouted bed drying on inert particles: Evaluation of particle size distribution of recovered, accumulated and elutriated powders. *Drying Technology*, 38(13):1709-1720, 2019.
- BARROS, J. P. A. A.; FREIRE, J. T. Análise do balanço de massa e da distribuição das partículas do pó na secagem de pasta em leite de jorro. In: COTIAN, L. F. P. *Engenharias, ciência e tecnologia*. Ponta Grossa/PR: Atena Editora, v.1, p.1-17, 2019.
- BRAGA, M. B.; ROCHA, S. C. S. Drying of milk-blackberry pulp mixture in spouted bed. *The Canadian Journal of Chemical Engineering*, 91(11):1786-1792, 2013.
- BRASIL. Ministério da Agricultura, Pecuária e Abastecimento. Instrução normativa N° 46, de 22 de novembro de 2016. Available in: <[https://www.in.gov.br/materia/-/asset\\_publisher/Kujrw0TZC2Mb/content/id/21295271/do1-2016-12-07-instrucao-normativa-n-46-de-22-de-novembro-de-2016-21295017](https://www.in.gov.br/materia/-/asset_publisher/Kujrw0TZC2Mb/content/id/21295271/do1-2016-12-07-instrucao-normativa-n-46-de-22-de-novembro-de-2016-21295017)>. Access in: April 19, 2023.
- BRASIL. Ministério da Agricultura, Pecuária e Abastecimento. Instrução Normativa MAPAN° 25. Off Gaz Bras 2009. Available in: <<https://www.diariodasleis.com.br/tabelas/211809.pdf>>. Access in: January, 03 2023.
- BRITO, R. C. et al. Drying of particulate materials in draft tube conical spouted beds: Energy analysis. *Powder Technology*, 388:110-121, 2021.
- DANTAS, T. N. P. et al. Study of model application for drying of pulp fruit in spouted bed with intermittent feeding and accumulation. *Drying Technology*, 36(11):1349-1366, 2018.
- DEHNAVAR, S.; SOURI, M. K.; MARDANLU, S. Tomato growth responses to foliar application of ammonium sulfate in hydroponic culture. *Journal of Plant Nutrition*, 40(3):315-323, 2017.
- DUARTE, C. R.; MURATA, V. V.; BARROZO, M. A. S. A Study of the fluid dynamics of the spouted bed using CFD. *Brazilian Journal of Chemical Engineering*, 22(2):263-270, 2005.
- ESTIATI, I. et al. Influence of the fountain confiner in a conical spouted bed dryer. *Powder Technology*, 356:193-199, 2019.
- FERRAZ, R. L. S. et al. Physiological adjustments, fiber yield and quality of colored cotton BRS Topázio cultivar under leaf silicon sprayin. *Ciência e Agrotecnologia*, 45:e005721, 2021.
- GINIFAB. Transferidor online. 2021. Available in: <[https://www.ginifab.com/feeds/angle\\_measurement/online\\_protractor\\_en-us.php](https://www.ginifab.com/feeds/angle_measurement/online_protractor_en-us.php)>. Access in: April 24, 2023.
- GONG, Z. et al. Spray drying and agglomeration of instant bayberry powder. *Drying Technology*, 26(1):116-121, 2008.
- MEDEIROS, M. F. D. et al. Drying of pulps of tropical fruits in spouted bed: Effect of composition on dryer performance. *Drying Technology*, 20(4-5):855-881, 2002.
- MUJUMDAR, A. S. *Handbook of industrial drying*. 4th Edition. Fourth Edition. CRC Press. 2014. 1348p.
- OLAZAR, M. et al. Stable operation conditions for gas-solid contact regimes in conical spouted beds. *Industrial & Engineering Chemistry Research*, 31(7):1784-1792, 1992.
- PASSOS, M. L.; MUJUMDAR, A. S. Effect of cohesive forces on fluidized and spouted beds of wet particles. *Powder Technology*, 110(3):222-238, 2000.
- PEREIRA, N. R.; GODOI, F.; ROCHA, S. C. S. Drying of starch suspension in spouted bed with inert particles: Physical and thermal analysis of product. *Drying Technology*, 28(11):1288-1296, 2010.
- ROCHA, S. C. S. et al. Drying of tropical fruit pulps: Spouted bed process optimization as a function of pulp composition. *Drying Technology*, 29(13):1587-1599, 2011.
- ROCHA, S. C. S.; DOMID, M. W.; MARQUES, A. M. M. Liquid-particle surface properties on spouted bed coating and drying performance. *The Canadian Journal of Chemical Engineering*, 87(5):695-703, 2009.
- SAN JOSÉ, M. J. et al. Solid cross-flow into the spout and particle trajectories in conical spouted beds. *Chemical Engineering Science*, 53(20):3561-3570, 1998.
- SANTOS, K. G. et al. CFD simulation of spouted bed working with a size distribution of sand particles: Segregation aspects. *Material Science Forum*, 899:95-100, 2017.
- SANTOS, K. G. et al. Spouting behavior of binary particle mixtures of different densities: Fluid dynamics and particle segregation. *Particuology*, 42:58-66, 2019.
- SANTOS, K. G. et al. Spouting of bidisperse mixture of particles: A CFD and experimental study. *Drying Technology*, 30(11-12):1354-1367, 2012.
- SANTOS, K. G.; MURATA, V. V.; BARROZO, M. A. S. Three-dimensional computational fluid dynamics modeling of spouted bed. *The Canadian Journal of Chemical Engineering*, 87(2):211-219, 2009.
- SOURI, M. K.; HATAMIAN, M. Aminocheletes in plant nutrition: A review. *Journal of Plant Nutrition*, 42(1):67-78, 2019.

- SOUZA, S. L. et al. Stability of cashew apple juice in powder dehydrated in spouted bed. *Revista Brasileira de Engenharia Agrícola e Ambiental*, 20(7):678-682, 2016.
- SUKUNZA, X. et al. A Model for predicting the performance of a batch fountain confined spouted bed dryer at low and moderate temperatures. *Powder Technology*, 405:117506, 2022.
- VIEIRA, G. N. A. et al. Real-time monitoring of milk powder moisture content during drying in a spouted bed dryer using a hybrid neural soft sensor. *Drying Technology*, 37(9):1184-1190, 2019.
- WESTERGAARD, V. *Milk powder technology: Evaporation and spray drying*. 5th ed. Edited by Niro A/S. 2004. 337p.